Statistical Study of Chorus Modulations by Background Magnetic Field and Plasma Density

Zhiyang Xia[1], Lunjin Chen[1], and Wen Li[2]

Zhiyang Xia, Department of Physics, University of Texas at Dallas, Richardson, Texas, USA 75080 (Zhiyang.Xia@utdallas.edu)

[1]Department of Physics, University of Texas at Dallas, Richardson, Texas, USA

[2]Center for Space Physics, Boston University, Boston, MA, USA

Abstract. In this study, we use observations of THEMIS and Van Allen Probes to statistically study the modulations of chorus emissions by variations of background magnetic field and plasma density in the ultra low frequency range. The modulation events are identified automatically and divided into three types according to whether the chorus intensity is correlated to the variations of magnetic field only (Type B), plasma density only (Type N) or both (Type NB). For THEMIS observations, the occurrences of the types B and N are larger than type NB, while for Van Allen Probes observations most events are Type N. The chorus intensity is mostly correlated to the magnetic field strength negatively and plasma density positively. Modulation event occurrences peak at the dawn sector. The chorus intensity tends to increase when the magnitude of the magnetic field perturbation increases, but little dependence on the amplitude of plasma density perturbation is found.

1. Introduction

Whistler-mode chorus emissions in the magnetosphere are right-hand polarized electromagnetic waves generated near the geomagnetic equator outside the plasmasphere [?????]. The chorus waves are usually separated into two frequency bands: the lower band from 0.1 to 0.5 f_{ce} and the upper band from 0.5 to 0.8 f_{ce}, where f_{ce} is the equatorial electron cyclotron frequency [???]. The excitation of chorus waves is generally believed to involve cyclotron resonance with anisotropic (nonuniform temperature distribution in different directions) electrons that are usually injected from the plasma sheet into the inner magnetosphere during geomagnetically active times [???]. The interactions between chorus waves and particles are very important to the magnetospheric dynamics, including acceleration of electrons to relativistic energy level through energy diffusion [??????] and precipitation of energetic electrons through pitch angle scattering [???]. The precipitating electrons can penetrate into the atmosphere and produce both diffusive [e.g., ???] and pulsating auroras [e.g., ????].

Statistical studies indicate that the intensity and occurrence of chorus waves usually increase under higher geomagnetic activity levels [???] and around the dawn sector (between midnight and noon) [??????]. A recent study also shows a strong dependence of chorus wave intensity on the solar wind parameters: the intensity increases during the periods of higher solar wind speed and southward interplanetary magnetic field [?]. The wave power spectra of chorus waves are often observed as on-off discrete elements with a time scale of about a tenth to a few tenths of seconds [?]. Those discrete elements merge together on a timescale from a few seconds to a few minutes, over which the averaged

intensity can be modulated by the variations of background magnetic field and plasma density [??????]. One primary source of the oscillations of background magnetic field and plasma density is Pc 4-5 ultra low frequency (ULF) waves, which were reported to modulate the chorus intensity in both large L-shell (8 to 12) region [?] and the inner magnetosphere [?]. In these two studies, the intensities of chorus waves show a positive correlation with plasma density and a negative correlation with the background magnetic field. The negative correlation between chorus intensity and plasma density in the absence of ULF waves has also been observed [?]. The modulated chorus emission can lead to modulated electron precipitation and the consequent pulsating aurora [??]. Understanding the chorus modulation is of importance to interpret the process of whistler mode wave excitation and the characteristics of pulsating aurora.

Despite existing event studies, the statistical relationship between fluctuations of magnetic field and density and the variation of chorus emission intensity remains to be explored. In this study, we use roughly 41 satellite-year observation in the inner magnetosphere to build a database of chorus modulation events and statistically study the relationships between the chorus emissions and perturbations of background magnetic field and plasma density. The organization of the paper is as follows. Section 2 introduces the THEMIS and Van Allen Probes satellites and corresponding instruments used. Section 3 describes the methods to automatically identify the chorus modulation events and to sort the events into different categories. Section 4 shows the occurrences and spatial distributions of different types of modulation events, and Section 5 gives a quantitative analysis of the relationship between the chorus intensity and amplitudes of background magnetic field and plasma density perturbations.

2. Spacecraft and Instruments

The Time History of Events and Macroscale Interactions during Substorms (THEMIS) mission is a constellation of five identically-instrumented satellites, which started in February 2007. Three of the satellites (THA, THD, and THE) are inner probes in nearly equatorial orbits with apogees of 10-13 R_E and perigees below 2 R_E [**?**], suitable to observe chorus waves outside the plasmasphere. The Fluxgate Magnetometer (FGM) [**?**] measures the background magnetic fields and their low-frequency fluctuations (up to 64 Hz). The Electric Field Instrument (EFI) measures three components of electric fields as well as individual sensor potentials, providing onboard and ground-based estimate of spacecraft floating potential and plasma density [**??**]. The Search Coil Magnetometer (SCM) [**??**] provides the measurements of three components of wave magnetic fields with a frequency range from 0.1 Hz to 4 kHz. The waveforms measured by EFI and SCM are digitized and processed by the Digital Fields Board (DFB) [**?**] and finally transformed into two types of spectral products: filter bank data (FBK) and Fourier power spectra (FFT). The filter bank data are meant for survey-type monitoring of wave power, which has broad frequency bands and relatively low time resolution. The THEMIS wave data used in this study is the FBK magnetic spectra.

The Van Allen Probes (or Radiation Belt Storm Probes (RBSP)) [**?**] consist of two satellites with identical instruments with nearly similar near-equatorial highly elliptical orbits with perigee about 620 km and apogee about 5.8 R_E. The Electric and Magnetic Field Instrument Suite and Integrated Science (EMFISIS) [**?**], equipped with a triaxial fluxgate magnetometer (MAG) and a triaxial AC magnetic search coil magnetometer (MSC), can provide the measurement of wave magnetic field in frequency range between

10 Hz and 400 kHz as well as the background magnetic field. The Electric Field and Waves Suite (EFW) [**?**], consisting of 4 spin-plane electric field antennae and 2 spin-axis tubular extendable booms, can provide not only the measurement of the electric field but also estimation of cold plasma densities above 10 cm^{-3} from spacecraft potential. Also, the EMFISIS Upper Hybrid resonance (UHR) lines can help to calibrate empirical plasma density-potential formula and improve the measurement of plasma density [e.g., **?**].

In this study, 10-year measurement of the three inner THEMIS satellites from 2008/01/01 to 2017/12/31 and 5.5-year measurement of the two Van Allen Probe satellites from 2012/09/15 to 2018/05/30 are used. In total, roughly 41 satellite-year measurement is used.

3. Identification of Modulation Events

In this section, we first introduce automatic detection of the modulation events from the observations of THEMIS and Van Allen Probes. The detection is achieved by calculating the two correlation coefficients: C_B between the background magnetic field, B_0, and logarithm value of the chorus wave root mean square amplitude, $\log B_w$, and C_N between the background plasma density N_0 and $\log B_w$. The value of B_w is the square root of the integration of the wave magnetic field spectral density over the frequency band from 0.1 to 0.8 electron cyclotron frequency f_{ce}. Calculation of the correlation coefficients is done over time intervals with high chorus wave amplitude outside the plasmasphere. First, we only perform the detection procedure outside the plasmasphere, which can be achieved by excluding the observation with corresponding plasma density larger than 10 cm^{-3}. Second, we select time intervals (with duration T_e) when the wave magnetic field amplitude B_w is at least twice the background value (which is obtained from the daily median value of

B_w with gradient of $log_{10}(B_w) < 0.02$ nT). Third, for the selected intervals with duration T_e longer than 36 seconds, we calculate the two correlation coefficients C_B and C_N in the time window of $2T_e$ (extending the identified T_e interval backward and forward by 0.5 T_e respectively). The coefficient calculation over the extended interval ensures that a high correlation coefficient really corresponds to a modulation event of interest. Finally, the time intervals with the absolute value of either C_B or C_N larger than 0.6 are recognized as modulation events. The minimum time window of 36 seconds is used because this time period lies in the ULF Pc 3 and Pi 1 bands and because this time period is a common multiple of the sampling periods of the wave data used of the two satellite missions, 4 seconds for THEMIS FBK data and 6 seconds for Van Allen Probe EMFISIS data.

According to the values of C_B or C_N, we sort the modulation events into 3 types and 8 subtypes. The three types are Type B with only high C_B absolute value; Type N with only high C_N absolute value; Type NB with both high C_B and C_N absolute values. For Type B and Type N, there are subtypes B^+ and N^+ with positive C_B and C_N values respectively and subtypes B^- and N^- with negative C_B and C_N respectively. For Type NB, the four subtypes are N^+B^+ with both positive C_B and C_N; N^-B^+ with positive C_B and negative C_N; N^+B^- with negative C_B and positive C_N; N^-B^- with both negative C_B and C_N. Examples of the eight subtypes of modulation events observed by THEMIS are shown in Figures 1a-1h. For each subplot, the upper panel shows the variations of B_0 (blue line) and N_0 (red line) while the lower panel shows the magnetic power spectrum density (colored spectrum) and the variation of B_w (red line). The white solid, dashed and dot-dash lines denote the variations of f_{ce}, $0.5f_{ce}$ and $0.1f_{ce}$, respectively.

4. Distribution of Modulation Events

After surveying THEMIS observations from Jan 2008 to Dec 2017, a total of 50851 modulation events are identified. For Van Allen Probes observation from September 2012 to May 2018, 3795 modulation events are identified. Now we sort these events into three types and eight subtypes and analyze the spatial distribution of the modulation events and compare the occurrences of different types of modulation events. The panels on the left side of Figure 2 show those statistical results of the 50851 modulation events from the THEMIS observation. Figures 2a - 2d exhibit the spatial distribution of modulation event occurrence rate in the logarithm scale for all the modulation events, type B, type N and type NB events respectively. The occurrence rate here, for a given spatial bin in MLT and L, is calculated as the ratio of the total time interval of the identified modulation events inside this bin to the total dwell time of the satellite inside the same bin. For the MLT distribution of type B and NB events which both involve the modulation effect of the background magnetic field, the modulation event occurrence maximizes at the dawn sector and minimizes near the midnight. There also exists a secondary peak in the dusk sector. However, for the type N events that involve only the modulation by plasma density, the MLT distribution is relatively uniform, compared with that of type B and NB events. The radial distribution peaks at L = 11-12 and decreases as L decreases for type B and NB events, while for type N event, the radial dependence is weaker. For the region outside $L = 12$, few observations due to the limit of THEMIS orbit are made and thus information about the distribution of modulation events cannot be reliably obtained. Figure 2e shows how chorus modulation is divided among the different types. The portions of the three types of events are 39.9%, 43.1%, and 17.0% for type B, N and NB events respectively.

Most of the type B events are subtype B^- with negative C_B (29.6% of all the modulation events) while most of the type N events are subtype N^+ with positive C_N (33.3% of all the modulation events). For type NB events, the main subtype is N^+B^- (10.5%), which can be treated as the combination of subtype B^- and N^+. Those proportions suggest that the chorus wave amplitude is more likely modulated by background magnetic field with negative correlation or by the plasma density with positive correlation. These modulation relations are consistent with those of the ULF wave modulation events reported in the outer [**?**] and inner magnetosphere [**?**].

Besides the statistical study of THEMIS data, we also perform a similar analysis on the measurements of Van Allen Probes from September 2012 to May 2018. The statistical results of Van Allen Probes data are plotted in the right column of Figure 2. Due to the orbit of Van Allen Probes, most of the 3798 events are detected within $L =\sim 6$, which greatly supplement the THEMIS observation of the events mostly at the outer L-shell. From the distribution of the proportions of different types of events shown by Figure 2j, we can see that most of the modulation events (64.1%) are type N^+, with positively correlated plasma density only. Also, there is a considerable number of type N^- events (12.8%) while the portion of the combined other types corresponding to the background magnetic field variation is about 23%. This proportion distribution may be due to the fact that the Van Allen Probes travel in the spatial region of relatively small L where the perturbations of plasma density are more frequent than the perturbations of background magnetic field. Looking into the MLT distribution of event occurrence rate, most of the events occur uniformly over a broad region from pre-midnight to pre-dusk region. For the

radial distribution, most of the events occur near $L =\sim 6$ and the event number decreases as L decreases.

Combining the results of both THEMIS and Van Allen Probes measurements, at larger L shell region ($L > 10$), most of the modulation events take place around the dawn sector while for regions of small L shell ($L < 10$), the MLT distribution of the modulation events become more uniform. Both THEMIS and Van Allen Probes measurements indicate that the number of modulation events decreases as L decreases. The occurrence rate near $L = 6$ obtained from THEMIS measurement and Van Allen Probes measurement are very close ($\sim 10^{-3} - 10^{-2}$), which shows a consistency between the observations of the two satellite missions.

5. Effects of Density and Magnetic Field Perturbations' Amplitudes

We have demonstrated that the intensity of the chorus wave can be modulated by the perturbations of the background magnetic field and plasma density. For modulation events, the relation between the intensity of the chorus wave and the amplitudes of the oscillations also needs to be investigated quantitatively to better understand the mechanism of the modulation events. To achieve this goal, we find out the maximum amplitudes of the chorus waves for all the modulation events, calculate the standard deviations of the corresponding variations of background magnetic field and plasma density, and analyze the quantitative relation between the maximum wave amplitudes and the deviations.

Figures 3a and 3b show the relationship between the logarithm values of chorus wave amplitudes and the logarithm values of standard deviations of background magnetic field for events observed by THEMIS satellites with positive C_B (subtypes B^+, N^+B^+ and N^-B^+) and negative C_B (subtypes B^-, N^+B^- and N^-B^-) respectively. The chorus wave

amplitudes and the magnetic field standard deviations are normalized by the mean background magnetic field over the corresponding event interval. The blue dots stand for type B events with only background magnetic field modulation (subtype B^- in 3a and B^+ in 3b) while the black dots are type NB events with both background magnetic field and plasma density modulations (subtypes N^+B^+ and N^-B^+ in 3a; N^+B^- and N^-B^- in 3b). The blue and black solid lines are linear fitting lines for dots with corresponding colors and the dashed lines outline the boundaries of the corresponding 95% predicting intervals (obtained by $y \pm 2\Delta$, where y is the predicted value of the linear fit and Δ is the standard error for prediction). In Figure 3b, the dots of the two different colors concentrate near the corresponding fitting lines with correlation coefficients of 0.65 (blue dots) and 0.70 (black dots), which indicates strong positive correlations between the intensity of chorus wave and the standard deviations of background magnetic field. The two corresponding fitting lines in the figure denotes two relations of $B_w/B_0 = 10^{-2.07}(\sigma_B/B_0)^{0.57}$ and $B_w/B_0 = 10^{-2.10}(\sigma_B/B_0)^{0.57}$ for the blue and black dots, respectively. The correlations in Figure 3a are weaker with correlation coefficients of 0.51 (blue dots) and 0.37 (black dots) with two corresponding fitting lines denoting $B_w/B_0 = 10^{-2.39}(\sigma_B/B_0)^{0.48}$ and $B_w/B_0 = 10^{-2.65}(\sigma_B/B_0)^{0.34}$ for the blue and black dots, respectively. These positive correlations suggest that stronger oscillations of the background magnetic field (larger magnitude) tend to result in more intense chorus waves, especially for the events with negative C_B. Figures 3c and 3d show the relationship between the logarithm values of normalized chorus intensity and the logarithm values of normalized standard deviations of plasma density (normalized by the mean plasma density over the event interval) for events observed by THEMIS satellites with positive C_N (subtypes N^+, N^+B^+ and N^+B^-)

and negative C_N (subtypes N^-, N^-B^+ and N^-B^-) respectively. The red dots stand for type N events with only plasma density modulation (subtype N^+ in 3c and N^- in 3d) while the black dots are type NB events with both background magnetic field and plasma density modulations (subtypes N^+B^+ and N^+B^- in 3c; N^-B^+ and N^-B^- in 3d). The effect of plasma density oscillation amplitude on chorus intensity is not as significant as that of background magnetic field since the data dots distribute more uniformly and the correlation coefficients for Figures 3c and 3d are all very low (absolute values $<\sim 0.15$).

Figures 3e-3h show the analysis results for observations of the Van Allen Probes in the same format as Figures 3a-3d. The effect of magnetic field oscillation is noticeable (Figures 3e and 3f) but not as significant as that in Figure 3b due to lack of measurements of events with modulation by the magnetic field. The effect of plasma density is still very weak (Figures 3g and 3h) from the results of Van Allen Probes' observations. In sum, the results from these two magnetospheric satellites missions indicate the chorus intensity increases when the amplitude of background magnetic field perturbation increases, but does not show a clear dependence on the amplitude of plasma density perturbation.

6. Conclusions and Discussion

In this study, we use nearly ten years of observations of three THEMIS satellites (A, D, E) and over 5.5 years of observations of two Van Allen Probes (A, B) to statistically study the modulations of chorus emissions by background magnetic field and density oscillations. The modulation events are identified automatically by calculating the correlation coefficients between the magnetic field strength (and plasma density) and the chorus emission intensity (calculated by integrating the magnetic wave power spectral density from 0.1 to 0.8 electron cyclotron frequency f_{ce}). The modulation events are divided into three types

according to whether the chorus intensity is highly correlated to the variations of magnetic field strength (type B), plasma density (type N), or both (type NB). The three types are also sorted into eight subtypes according to the sign of correlation coefficients. The occurrence rates and the proportions of the three types of modulation events are analyzed. Finally, we analyze the relationships between chorus wave amplitudes and amplitudes of the magnetic field and plasma density perturbations, respectively. The conclusions are listed below:

1. The proportions of types B and N are comparable ($\sim 2/5$ of total events) and slightly larger than that of type NB ($\sim 1/5$) for the THEMIS observations, while for the Van Allen Probes observations at relatively smaller L-shell most of the events are type N.

2. The chorus intensity is mostly correlated to the magnetic field strength negatively and plasma density positively.

3. The occurrence rate of the modulation events is favored on the dawn sector for all the three types and at higher L-shell.

4. For the modulation events, chorus intensity is larger when the amplitude of the magnetic field perturbation is larger but has no clear dependence on the amplitude of plasma density perturbation.

We have also tested modulation event identification with a different critical C_N and C_B value (0.8) and the plasmapause identification with a different critical density (100 cm^{-3}). As a result of the two tests, the event number decreases and increases respectively. However, these do not affect our main conclusions about the spatial distribution of the modulation events and the relationship between the chorus intensity and the amplitude of the background parameter perturbations.

The linear theory [?] could partially explain the excitation of chorus waves especially for small amplitude chorus waves. As discussed in **??**, the mechanism of chorus modulation by compressional ULF waves corresponding to the linear growth rate can be decomposed as the changes of the ratio between the resonant electrons and the total electrons $R(V_R)$ ($V_R = \frac{\omega - |\Omega_e|}{k}$ is the nonrelativistic, parallel velocity of electrons that interact with whistler waves through the first order resonance, where ω is the wave frequency and Ω_e is the electron cyclotron frequency) as well as the electron anisotropy $A(V_R)$. The value of $R(V_R)$ is affected by both the electron density and the minimum resonant energy. The minimum resonant energy can be calculated by $E_{min} = \frac{B_0^2}{8\pi N_0}\frac{\Omega_e}{\omega}(1 - \frac{\omega}{\Omega_e})^3$ (Equation (1) in **?**). Consider a fixed value of $\frac{\Omega_e}{\omega}$, E_{min} increases (and thus the number of resonant electrons increases) as B_0^2/N_0 increases. This explains the reason that most type B events have negative values of C_B and the monotonic correlation between the chorus intensity and amplitude of the magnetic oscillation is significant. **?** also confirms that the growth rate increases monotonically as background magnetic field increases or decreases when the density ratio between total and hot electrons is much larger than 1 or close to 1, respectively. The effects of total electron density variation on the linear growth rate is more complex. As discussed in **?**, both density enhancement (DE) and depletion (DD) can increase the value of $R(V_R)$ and thus the linear growth rate. The DE can increase $R(V_R)$ by reducing E_{min} (and thus increasing the number of resonant electron), while the DD can increase $R(V_R)$ by reducing the total electron density. From our statistical result, the events with positive C_N are several times more often than the events with negative C_N. This indicates that the effect of N_0 on the number of resonant electrons is more important than the change of N_0 itself in the magnetosphere, especially in the inner

region ($L < 6$, shown by the Van Allen Probes results of a larger proportion of Type N^+ events than the THEMIS events). This complex effect of the total density may explain why there is no significant monotonic relationship between the chorus intensity and the amplitude of density perturbation. Another possible reason is the additional effect of the total electron density on $A(V_R)$. According to Equation 3 of **?**, the dependence of whistler wave growth rate on cold plasma density is non-monotonic, and the relation between the two strongly depends on the hot electron anisotropy and wave frequency. As a final remark, our statistical study here focuses on the dependence on wave amplitudes, while ignoring the effects of density and magnetic field modulation on wave frequency and wave polarization features, which are left for future investigation.

Acknowledgments. We acknowledge the support of NSF grants AGS-1405041 and 1702805, and the AFOSR grant of FA9550-16-1-0344. Wen Li gratefully thanks the NSF grant AGS-1847818, NASA grants NNX15AI96G and NNX17AG07G, and the Alfred P. Sloan Research Fellowship FG-2018-10936. The data of THEMIS and Van Allen Probes used in this paper are provided by Space Physics Data Facility (SPDF) https://spdf.gsfc.nasa.gov/.

References

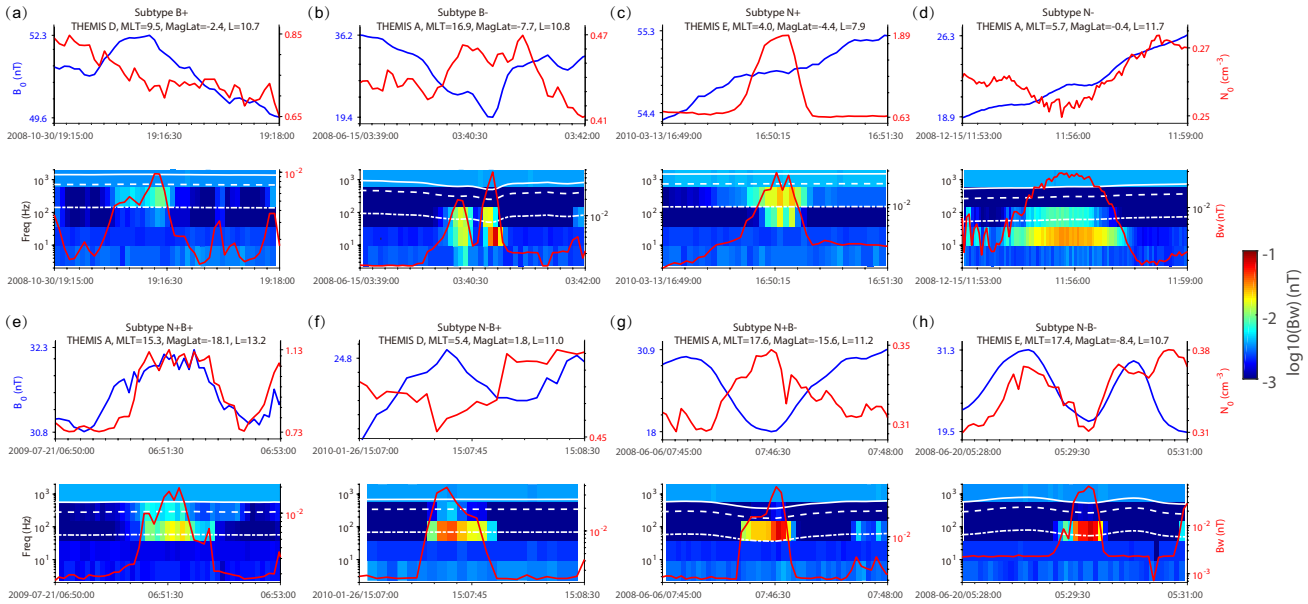

Figure 1. Representative events of the eight subtypes of chorus modulation events from the observations of THEMIS satellites. For each subplot, the upper panel shows the variations of the background magnetic field (blue line) and plasma density (red line) and the lower panel shows the magnetic wave spectrum overplotted with the variation of chorus wave root mean square amplitude B_w (red line) as well as the variations of f_{ce}, $0.5f_{ce}$ and $0.1f_{ce}$ (white solid, dashed, dash-dot lines).

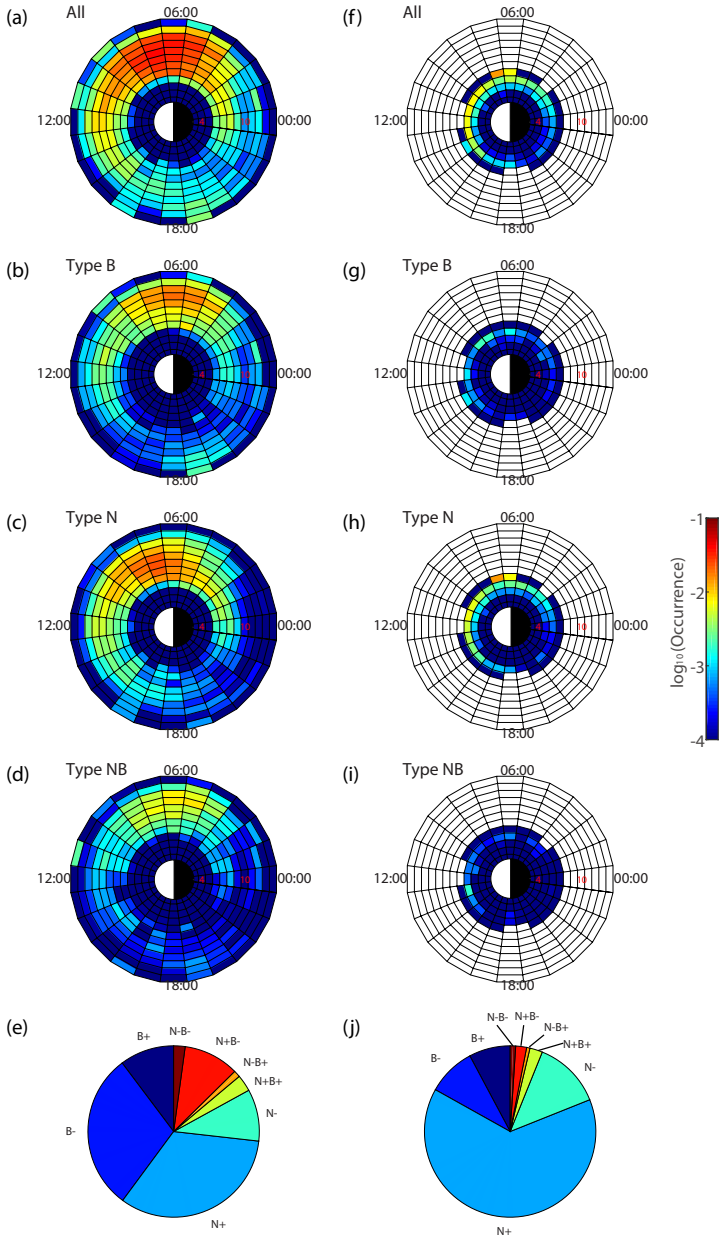

Figure 2. Spatial distribution of the occurrence rates of different modulation types and the proportions of different subtypes. The spatial distribution of modulation events numbers for all types (a), type B (b), type N (c) and type NB (d) respectively from THEMIS observation. (e): the proportion of different subtypes of events from THEMIS observation. (f) - (j) show similar content to (a) - (e) except for Van Allen Probes observation of modulation events.

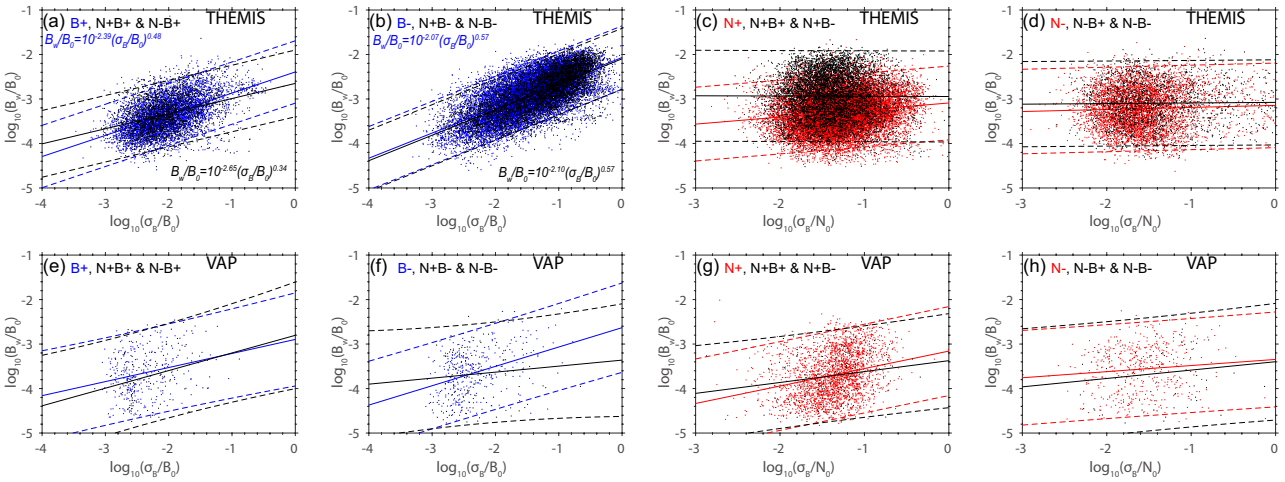

Figure 3. Relationship between the chorus intensity and the amplitudes of the perturbations of background magnetic field and plasma density for different types of chorus modulation events. (a) and (b) show relation between normalized chorus wave intensity (y axis) and normalized amplitude of background magnetic field perturbation (x axis) for events observed by THEMIS (blue: type B, Black: type NB) with (a) positive and (b) negative correlations, respectively. (c) and (d) show relation between normalized chorus wave intensity (y axis) and normalized amplitude of plasma density perturbation (x axis) for events observed by THEMIS (red: type N, Black: type NB) with (c) positive and (d) negative correlations, respectively. (e) - (f) show similar content to (a) - (d) except for Van Allen Probes observations. The solid lines are linear fitting lines for dots with corresponding colors and the dashed lines outline the boundaries of the corresponding 95% predicting intervals.

Figure 1.

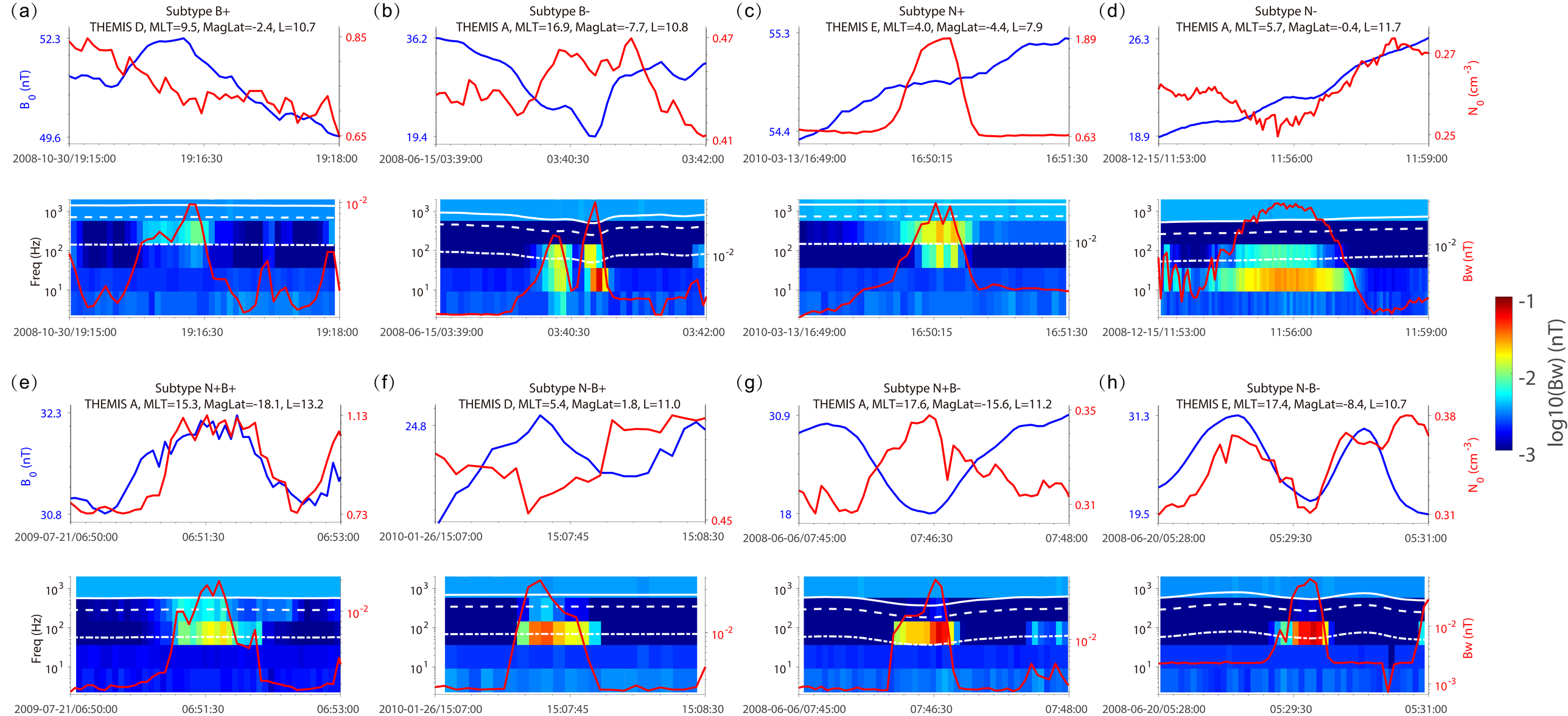
(a)
Subtype B+
THEMIS D, MLT=9.5, MagLat=-2.4, L=10.7
(b)
Subtype B-
THEMIS A, MLT=16.9, MagLat=-7.7, L=10.8
(c)
Subtype N+
THEMIS E, MLT=4.0, MagLat=-4.4, L=7.9
(d)
Subtype N-
THEMIS A, MLT=5.7, MagLat=-0.4, L=11.7
(e)
Subtype N+B+
THEMIS A, MLT=15.3, MagLat=-18.1, L=13.2
(f)
Subtype N-B+
THEMIS D, MLT=5.4, MagLat=1.8, L=11.0
(g)
Subtype N+B-
THEMIS A, MLT=17.6, MagLat=-15.6, L=11.2
(h)
Subtype N-B-
THEMIS E, MLT=17.4, MagLat=-8.4, L=10.7
B0 (nT)
N0 (cm-3)
Freq (Hz)
Bw (nT)
log10(Bw) (nT)

Figure 2.

(a)

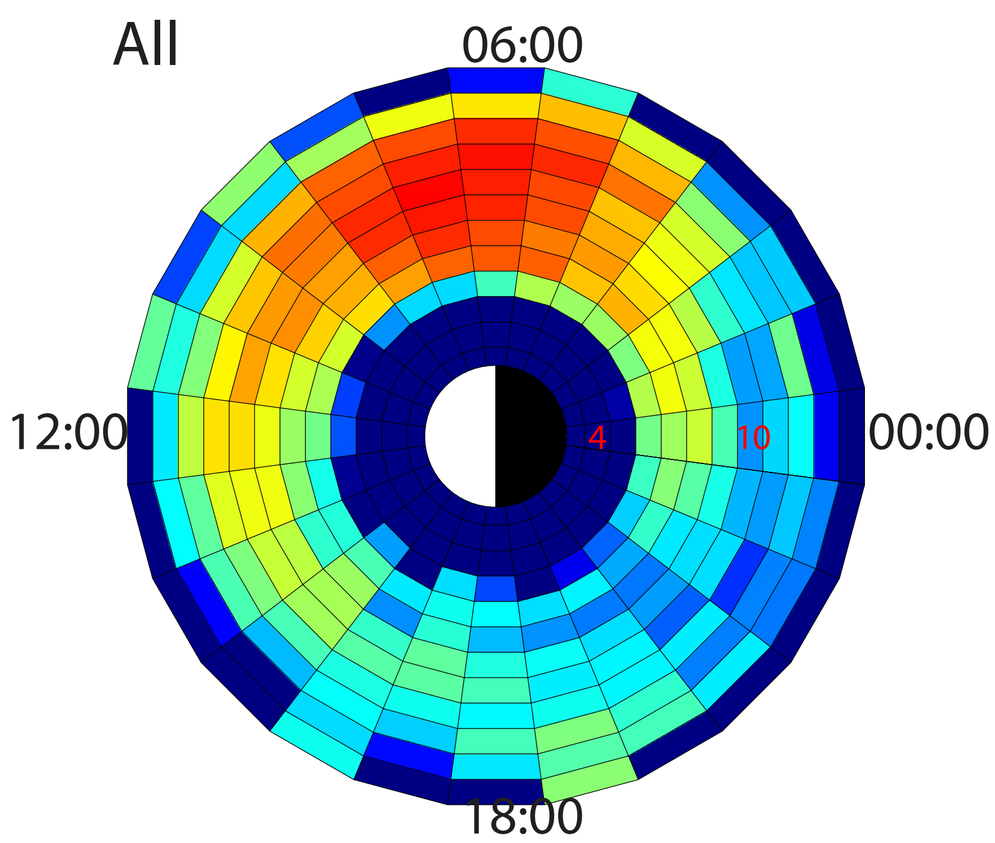
All
06:00
12:00
00:00
18:00
4
10

(b)

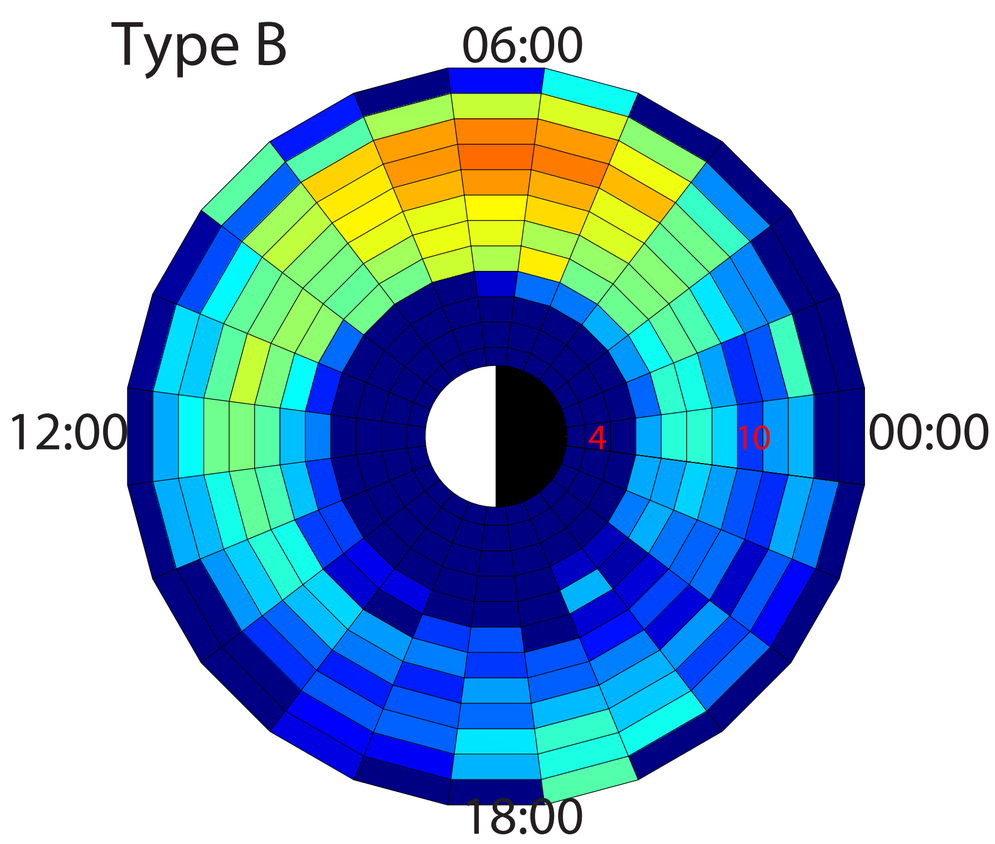
Type B
06:00
12:00
00:00
18:00
4
10

(c)

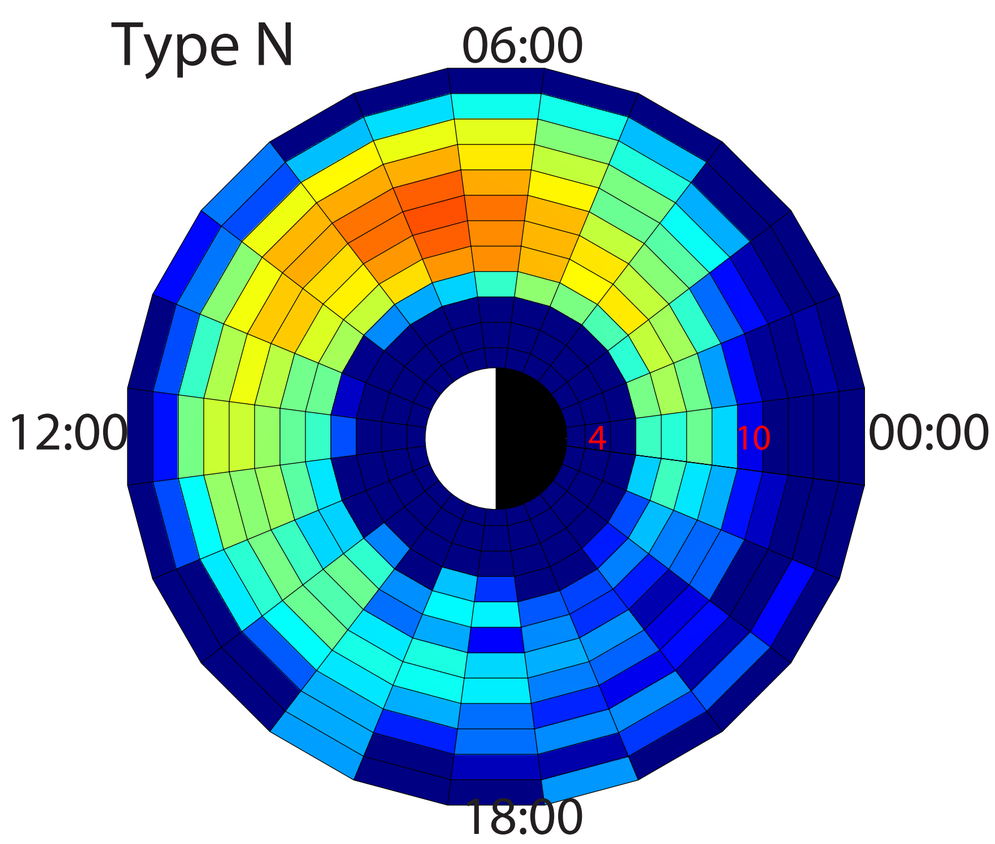
Type N
06:00
12:00
00:00
18:00
4
10

(d)

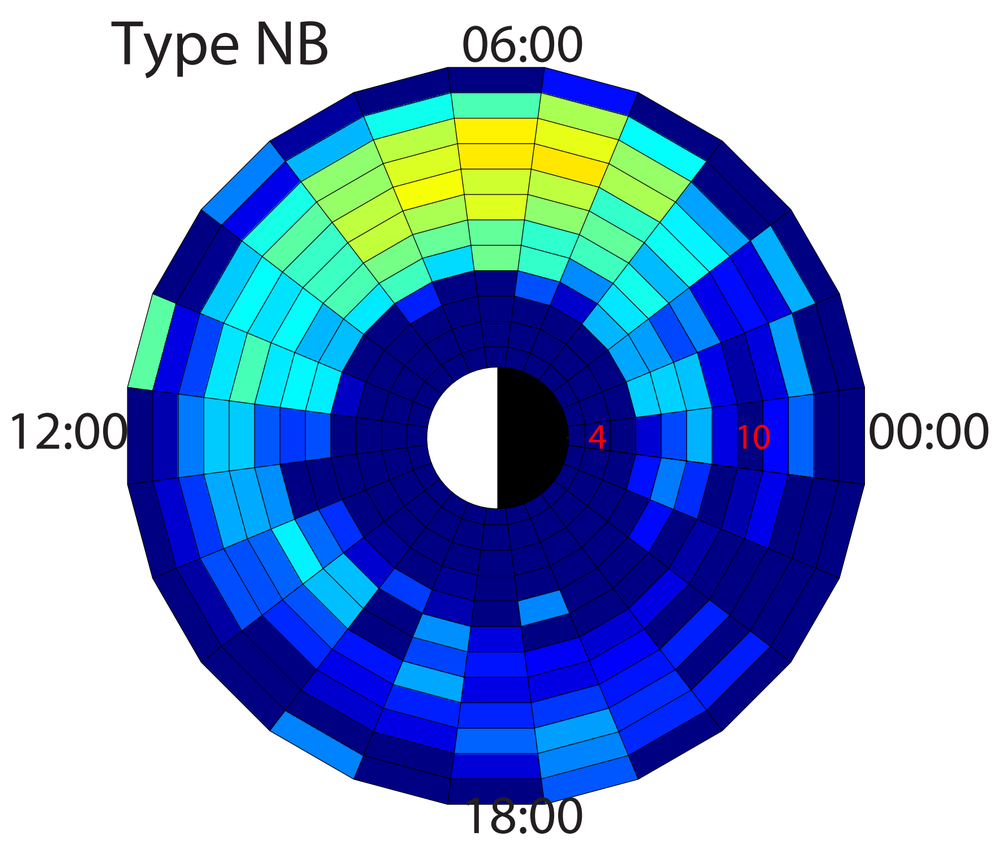
Type NB
06:00
12:00
00:00
18:00
4
10

(e)

B+
N-B-
N+B-
N-B+
N+B+
N-
B-
N+

(f)

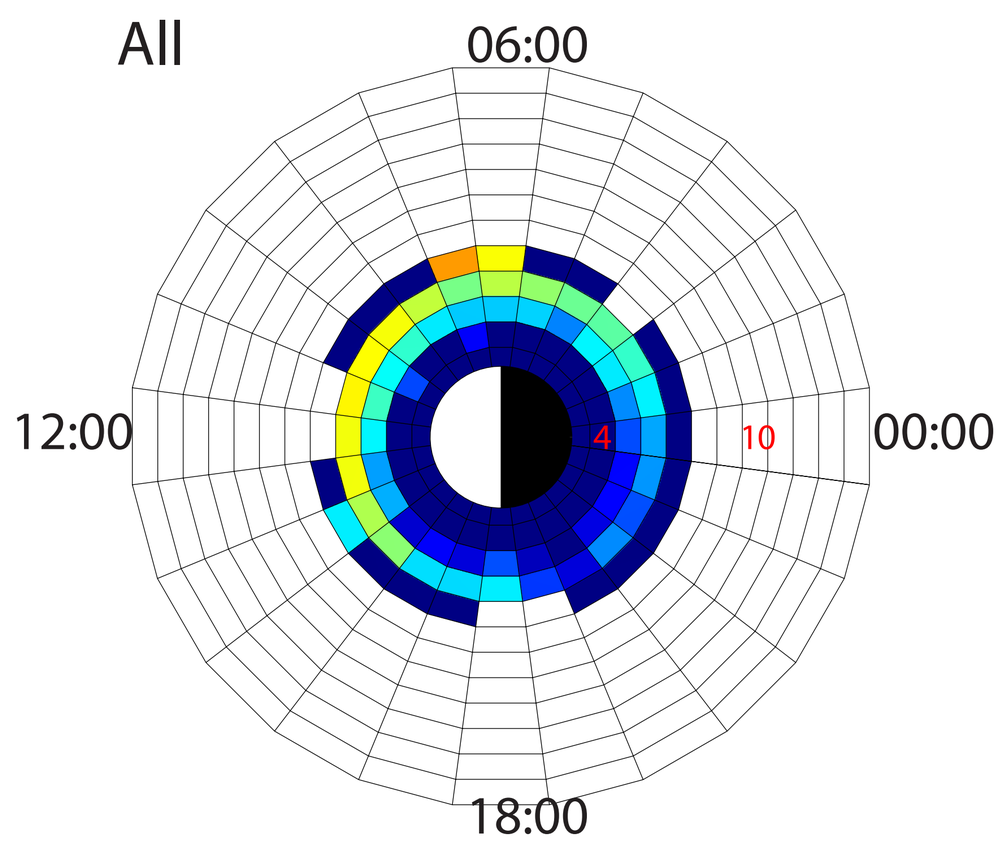
All
06:00
12:00
00:00
18:00
4
10

(g)

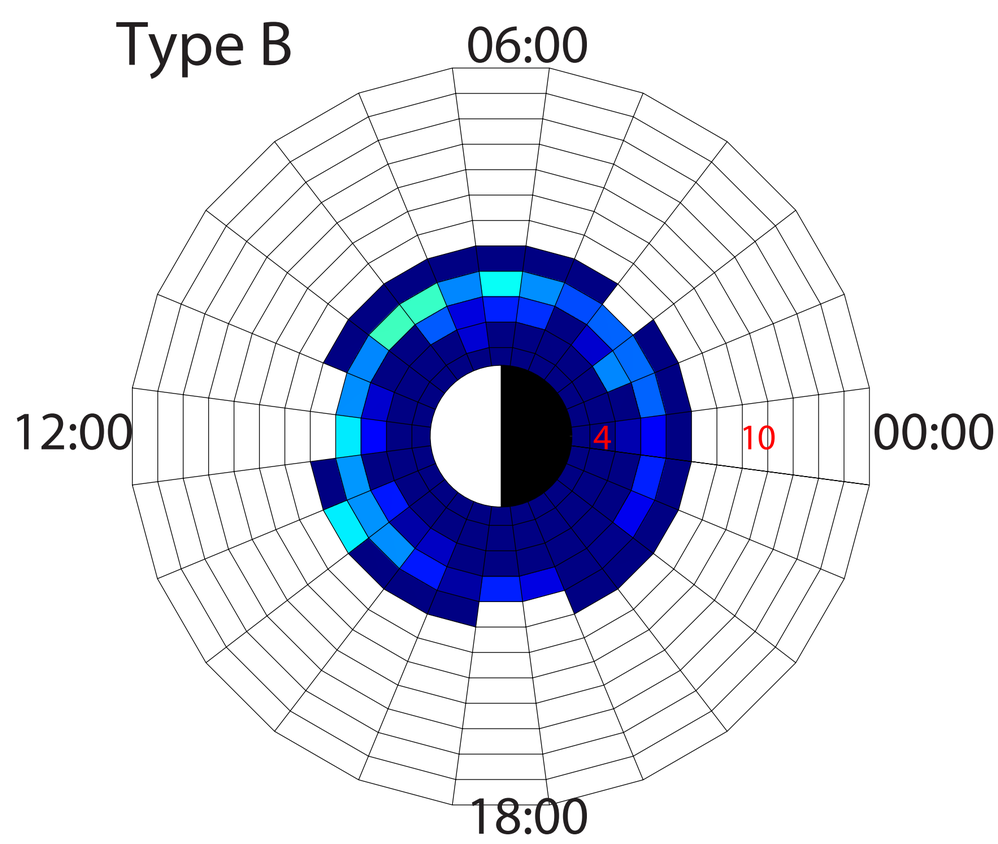
Type B
06:00
12:00
00:00
18:00
4
10

(h)

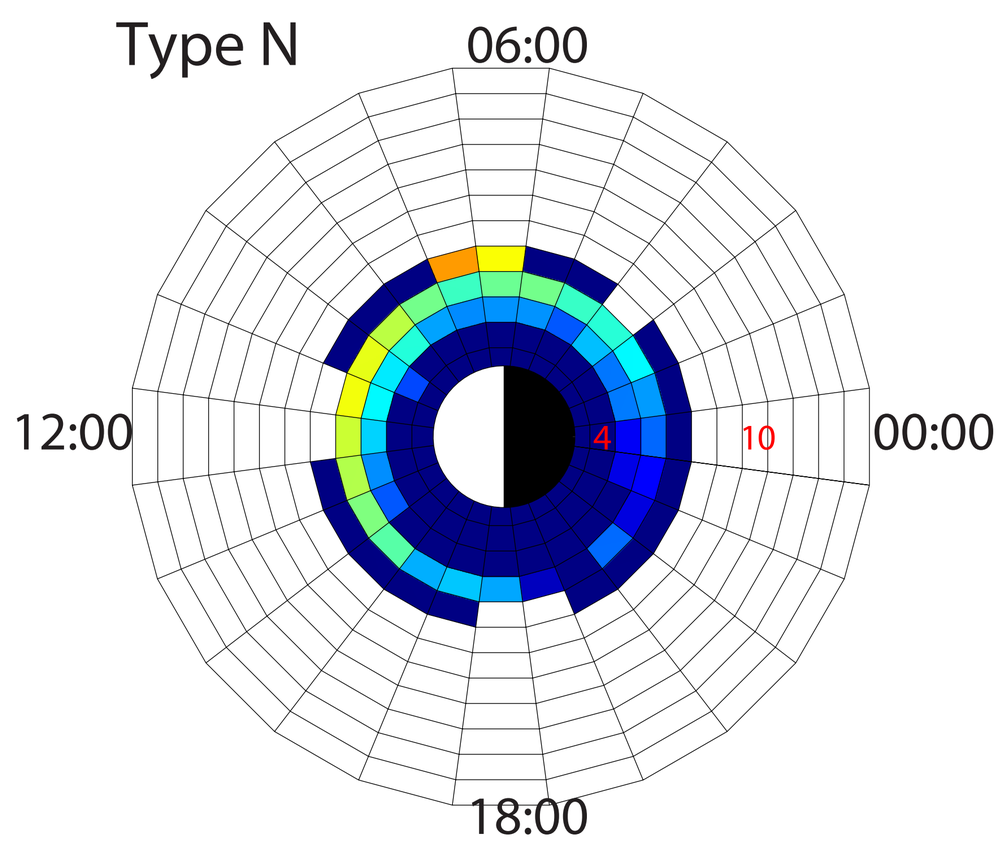
Type N
06:00
12:00
00:00
18:00
4
10

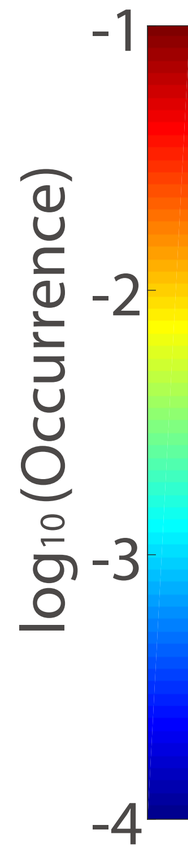
-1
-2
-3
-4
log10(Occurrence)

(i)

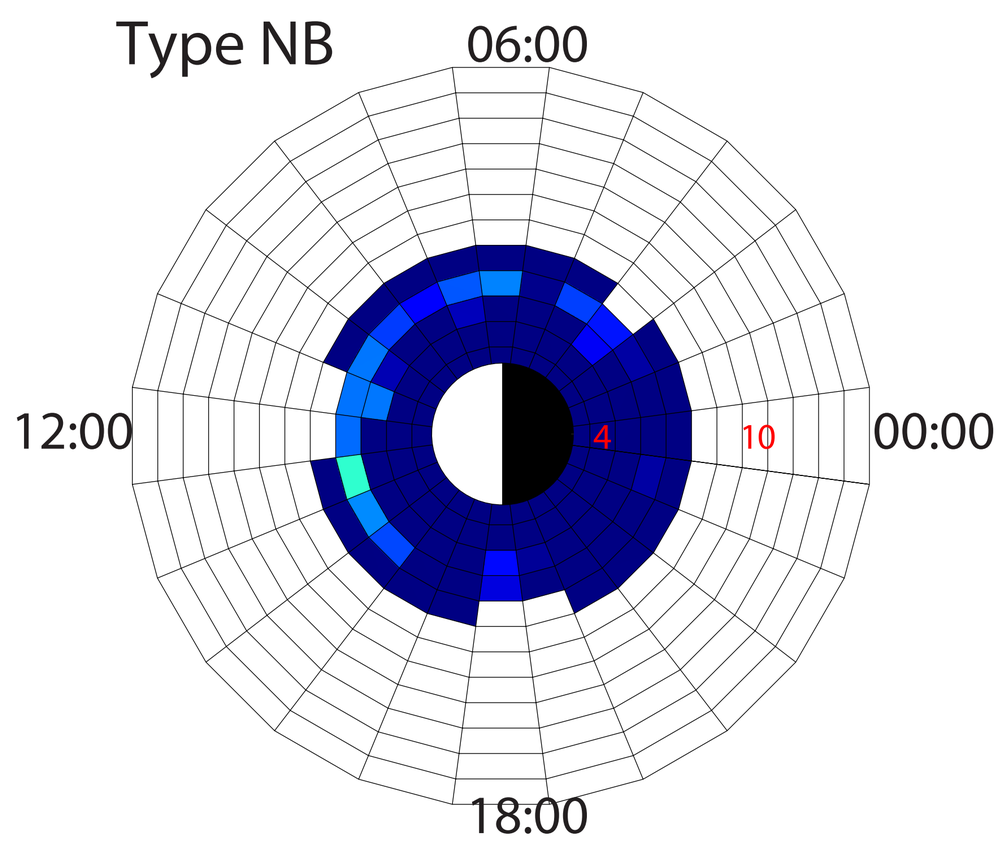
Type NB
06:00
12:00
00:00
18:00
4
10

(j)

N-B-
N+B-
N-B+
N+B+
B+
B-
N-
N+

Figure 3.

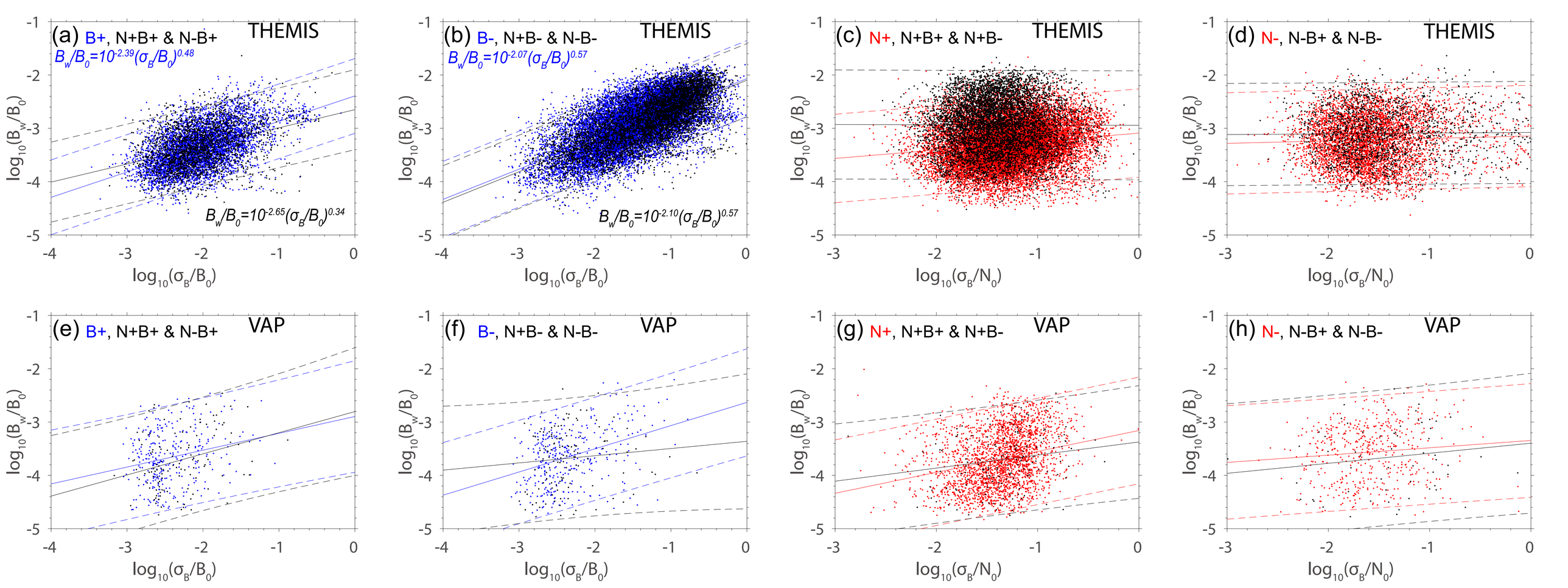
(a) B+, N+B+ & N-B+
THEMIS
$B_w/B_0=10^{-2.39}(\sigma_B/B_0)^{0.48}$
$B_w/B_0=10^{-2.65}(\sigma_B/B_0)^{0.34}$
(b) B-, N+B- & N-B-
THEMIS
$B_w/B_0=10^{-2.07}(\sigma_B/B_0)^{0.57}$
$B_w/B_0=10^{-2.10}(\sigma_B/B_0)^{0.57}$
(c) N+, N+B+ & N+B-
THEMIS
(d) N-, N-B+ & N-B-
THEMIS
(e) B+, N+B+ & N-B+
VAP
(f) B-, N+B- & N-B-
VAP
(g) N+, N+B+ & N+B-
VAP
(h) N-, N-B+ & N-B-
VAP
$\log_{10}(B_w/B_0)$
$\log_{10}(\sigma_B/B_0)$
$\log_{10}(\sigma_B/N_0)$